

Journal of Materials Chemistry C

Accepted Manuscript



This is an *Accepted Manuscript*, which has been through the Royal Society of Chemistry peer review process and has been accepted for publication.

Accepted Manuscripts are published online shortly after acceptance, before technical editing, formatting and proof reading. Using this free service, authors can make their results available to the community, in citable form, before we publish the edited article. We will replace this *Accepted Manuscript* with the edited and formatted *Advance Article* as soon as it is available.

You can find more information about *Accepted Manuscripts* in the [Information for Authors](#).

Please note that technical editing may introduce minor changes to the text and/or graphics, which may alter content. The journal's standard [Terms & Conditions](#) and the [Ethical guidelines](#) still apply. In no event shall the Royal Society of Chemistry be held responsible for any errors or omissions in this *Accepted Manuscript* or any consequences arising from the use of any information it contains.

Cation and Anion Ordering in $\text{Sr}_2\text{Si}_7\text{Al}_3\text{ON}_{13}$ Phosphors

Graham King,^{1*} Kunio Ishida,^{2*} Katharine Page,^{1,3} Yumi Fukuda,² Ariane Keiko Albessard,² Yasushi Hattori,² Ryosuke Hiramatsu,² Iwao Mitsuishi,² Aoi Okada,² Masahiro Kato,² and Noburu Fukushima²

¹ Lujan Neutron Scattering Center, Los Alamos National Laboratory, Los Alamos, New Mexico, 87545, USA

² Corporate Research and Development Center, Toshiba Corporation, 1, Komukai-Toshiba-cho, Saiwai-ku, Kawasaki 212-8582, Japan

³ Spallation Neutron Source, Oak Ridge National Laboratory, Oak Ridge, Tennessee, 37831, USA

*Corresponding authors

Abstract

A series of photoluminescent Ce^{3+} doped samples with compositions close to $\text{Sr}_2\text{Si}_7\text{Al}_3\text{ON}_{13}:\text{Ce}$ have been studied by neutron powder diffraction to determine the $\text{Si}^{4+}/\text{Al}^{3+}$ and $\text{N}^{3-}/\text{O}^{2-}$ site ordering. Contrary to a commonly held assumption that the edge sharing tetrahedral sites in this structure are occupied exclusively by Al^{3+} , we find a partial occupancy of Al^{3+} on these site but also an unexpected preference for Al^{3+} to occupy 2 other tetrahedral sites which are only corner sharing. From the crystal structures and local structures, as determined by pair distribution function (PDF) analysis, we also find evidence for alternating Si-Al site ordering within the edge sharing chains as well as dimerization of the Si^{4+} and Al^{3+} cations within these chains. The O^{2-} are found to be partially ordered onto 2 of the anion sites, although small amounts of O^{2-} are found on other sites as well. The cation and anion ordering found by neutron diffraction is supported by theoretical calculations. Understanding cation and anion ordering is essential for optimizing the photoluminescence properties of this promising class of phosphor materials.

1. Introduction

Phosphors for white light emitting diodes have been extensively studied recently because of the emerging need for energy saving devices. For practical applications such materials are required to have particular features such as high quantum efficiency under visible excitation and high thermal stability of luminescence. Silicon nitride compounds are a promising class of host materials due to their high chemical stabilities, their tendency to form rigid frameworks, and the favorable ligand field environment caused by nitrogen coordination.¹⁻⁷ Recently, several studies have reported desirable photoluminescent properties in a new structure type with the formula SrAlSi₄N₇. This material has been shown to exhibit good emissions properties when doped with Eu²⁺, Yb²⁺, or Ce³⁺.⁸⁻¹²

The SrAlSi₄N₇ structure is complex. It has space group symmetry *Pna2*₁ with 26 crystallographically unique positions all on general sites with multiplicities of 4. The formula can also be written as *A*₂*B*₁₀*X*₁₄ to reflect the number of unique sites in the structure. The two *A*-sites (gray spheres in Fig. 1) are occupied by Sr²⁺ and also contain the rare earth ions when the compound is doped to produce a phosphor. There can also be small amounts of vacancies present on the *A*-sites. The ten *B*-sites (blue and green tetrahedra in Fig. 1) contain the Si⁴⁺ and Al³⁺ cations, which are all tetrahedrally coordinated. Eight of the ten *BX*₄ tetrahedra share only corners with other *BX*₄ tetrahedra (blue tetrahedra in Fig. 1). The tetrahedra of the other two *B*-cations share edges with each other as well as corners to other *BX*₄ tetrahedra. These form chains of edge sharing tetrahedra along the *c*-axis of the structure (green tetrahedra in Fig. 1). The *X*-sites (red spheres in Fig. 1) are occupied by the anions, which are primarily N³⁻. However, it is very difficult to completely exclude oxygen during synthesis and most samples contain small amounts of O²⁻ on the *X*-sites as well. While the atomic positions for this structure type have already been determined using single crystal X-ray diffraction,¹³ the distributions of the cations and anions over the different sites is still not known.

It has not been established whether the Al³⁺ cations are ordered onto specific sites or randomly distributed among the *B*-sites. Since Si⁴⁺ and Al³⁺ are isoelectronic and only differ in *Z* by 1, they are essentially indistinguishable by X-ray diffraction. In several earlier papers on SrAlSi₄N₇ compositions it has been assumed that the Al³⁺ occupied the edge sharing sites, while the sites that are corner sharing are only occupied by Si⁴⁺.⁹⁻¹² Such an assumption makes sense in that the metal-metal distances within the edge sharing chains (~2.5 Å) are much shorter than those between corner sharing tetrahedra (~3.1-3.3 Å). From an electrostatic perspective, the lower valent Al³⁺ would preferentially occupy these sites to minimize cation-cation repulsion. However, no experimental evidence has been offered to support this assumption. The neutron scattering lengths of Si and Al are 4.15 and 3.45 fm, respectively, offering an adequate level of contrast to help in determining the site ordering. One study did report using neutron diffraction to try to establish the Al locations, but the results were inconclusive.⁸

The locations of oxygen atoms, which are almost inevitably present in any real samples, are an issue which has not yet been addressed in the literature at all. N^{3-} and O^{2-} are also indistinguishable by X-ray diffraction. Fortunately, the neutron scattering lengths of N and O, 9.36 and 5.80 fm respectively, are quite different. This allows for the determination of the site ordering even for small concentrations of O.

In this study we have determined the Si/Al and N/O site ordering in a series of Ce^{3+} doped samples with compositions close to $\text{Sr}_2\text{Si}_7\text{Al}_3\text{ON}_{13}$ using neutron powder diffraction. We have also identified several local structure features that are impacted by this ordering. These results are supported by density functional theory calculations. Our results show a partial ordering onto both the *B*-sites and *X*-sites, which affects the band structure of the materials family.

2. Methods

Eighteen samples were prepared using standard solid state methods. The samples each had slightly different compositions and were prepared using slightly varied synthesis conditions. The compositions were all close to the nominal composition of $\text{Sr}_2\text{Si}_7\text{Al}_3\text{ON}_{13}:\text{Ce}$. The Ce doping level at the *A*-site varied from 2% to 6%. The compositions were determined by inductively coupled plasma atomic emission spectroscopy. Time-of-flight neutron total scattering data was collected for all samples on either the HIPD or NPDF neutron diffractometers at the Lujan Neutron Scattering Center of Los Alamos National Laboratory at 298 K. Rietveld refinements were carried out using the GSAS/EXPGUI software package.^{14,15} The pair distribution functions (PDFs) were generated using the program PDFgetN with a Q_{max} of 30 \AA^{-1} and the reverse Monte Carlo modeling of the PDFs was completed with the RMCProfile program.^{16,17}

The electronic structure of the host materials was calculated by density functional theory (DFT) within the local density approximation and the plane-wave pseudo-potential method¹⁸⁻²⁰. All the calculations were performed by the PHASE code in non-magnetic states. We took uniform $2 \times 2 \times 2$ *k*-points and the plane wave energy cut-off values are 70 Ry for wavefunction and 220 Ry for charge density. A material composition of $\text{Sr}_2\text{Si}_7\text{Al}_3\text{ON}_{13}$ is assumed in all the calculations, which utilize the 104 atom unit cell shown in Fig. 1. The atomic coordinates and the lattice parameters were optimized for a single unit cell. The total energy is -870.14 hartree in the lowest energy case with $a = 11.95 \text{ \AA}$, $b = 21.55 \text{ \AA}$, and $c = 5.02 \text{ \AA}$. These values are 1-2% larger than the experimental values and thus we consider that the calculated results are reliable in the present system.

3. Results and Discussion

3.1 Rietveld Refinements. The structures of all eighteen samples were determined by Rietveld refinements of the neutron powder diffraction data. The starting coordinates used were those obtained from a single crystal X-ray diffraction experiment on a sample of similar composition. During the refinements the lattice parameters, zero point errors, backgrounds, profile functions, atomic coordinates, atomic displacements parameters (ADPs), absorption corrections, and fractional occupancies were refined. For each refinement only three independent ADPs were refined, one for all the *A*-cations, one for all the *B*-cations, and one for all the *X*-anions. This was done to reduce the number of variables in the refinement and to prevent correlations between the ADPs and the fractional occupancies of particular sites. The occupancies of the Si and Al sites were refined for all samples with the restriction that the occupancy of every *B*-site remained 1. The occupancies of the *X*-sites were also refined in a similar manner, but only for those samples which had larger O concentrations. While the atomic coordinates were slightly different for all samples, there were no major differences among any of the samples. The refined coordinates of one representative sample are given in Table 1 in order to identify the site numbering scheme used in this work. A fit to the neutron diffraction pattern for the same sample is shown in Figure 2 as a representative example of a refinement result.

3.2 Si⁴⁺/Al³⁺ Ordering. There are ten *B*-sites in the structure which contain the Si⁴⁺ and Al³⁺ cations. Eight of these sites belong to *BX*₄ tetrahedra which only share corners with other *BX*₄ tetrahedra (*B1*-*B8*), while the other two sites (*B9* and *B10*) are part of *BX*₄ tetrahedra which share both corners and edges to form chains of edge sharing tetrahedra along the *c*-axis. The refinement of the Si/Al site occupancies produced the same general trends for all samples. The overall conclusion is that the Al are partially ordered onto 4 sites. These include the *B9* and *B10* sites, but also include two other corner sharing only sites.

The *B9* and *B10* edge sharing sites were always found to have significant concentrations of Al on them, although they were almost never fully occupied despite there being more than enough Al in all samples for this to be the case. Another important finding was that the *B9* and *B10* sites did not have the same concentrations of Al, but often the *B10* site had much more than the *B9* site. Amongst the different samples, the Al fractional occupancy on the *B9* site ranged from 0.03-0.57 and had an average concentration of 0.41. The *B10* Al occupancy ranged from 0.44-1.00 and had an average of 0.67. In some samples it was found that the *B9* and *B10* had similar Al concentrations of roughly one half each, while in other samples the *B9* site had only a small concentration of Al while the *B10* site was fully occupied or close to fully occupied. This would suggest that there may be some kind of Si-Al cation ordering within the edge sharing chains in these samples. This point will be addressed in more detail later.

Significant concentrations of Al were also found on the *B1* and *B7* sites. The Al occupancy of the *B1* site ranged from 0.09-0.81 and had an average occupancy of 0.54. The *B7* site had a wide variation, with refined values of Al occupancy ranging all the way from 0 to 1.

However, for most samples the refinements produced values near the average of 0.58. The *B*6 sites also refined to have some Al on them, although the amount was always small. The *B*2, *B*3, *B*4, *B*5, and *B*8 sites usually refined to be completely occupied by Si or in a few cases they had very small amounts of Al present. Since the neutron scattering contrast between Si and Al is not large the estimated standard deviations (ESDs) for the occupancies of the *B*-sites were usually 0.04 or 0.05. While this is a large enough error to prevent precise determination of the site occupancies, it is still small enough to draw general conclusions. The fact that similar results were found for a large number of different samples measured on two different instruments increases our confidence in the validity of these results.

In order to reveal which sites Al³⁺ prefers electronic structure calculations were performed on the host material varying the occupancy of the Al/Si sites. Since the synthesis process employed in the present study is regarded as being in thermal equilibrium, we consider that the primary phase in the samples is that with the lowest-energy configuration. Referring to the experimental results described above, such configuration is found among those in which Al occupies three of the four *B*1 (corner-sharing only), *B*7 (corner-sharing only), *B*9 (corner and edge-sharing), and *B*10 (corner and edge-sharing) sites. The results of the calculations show that the lowest-energy state is realized when *B*1, *B*7, and *B*10 are occupied by Al, which supports the experimental finding that while the edge sharing chains contain considerable amounts of Al, they are not fully occupied by Al.

3.3 Dimerization within the Edge Sharing Chains. The refined occupancies of the *B*9 and *B*10 sites suggests that for some samples there may be a pattern of alternating Si and Al within the edge sharing chains. The refined metal-metal distances in the chains also indicate that there may be a dimerization of these *B*-cations. The crystal symmetry results in two *B*-*B* distances within the chains. In some samples these two distances were found to be nearly equal, both being around 2.48 Å. In other samples they were quite different. The differences were as large as 0.15 Å, giving *B*-*B* distances of ~2.41 Å and ~2.55 Å. Such short distances would imply that there is some sort of metal-metal bonding occurring. Interestingly, the samples which showed two different metal-metal distances are the same ones which showed a large difference between the *B*9 and *B*10 Al occupancies. This implies that differences in the metal-metal distances and cation ordering within the edge sharing chains may be correlated. These results suggest that there may be Si-Al ordering within these chains and that the cations dimerize to form Si-Al pairs.

These results bring up the question of why this intra-chain cation ordering and dimerization is found only in some of the samples, despite them all having similar compositions. One theory is that such ordering is occurring in all samples, there is just a difference in the correlation length such that it only appears in the long range average structures of some samples. It could be that small differences in material preparation or composition create differences in the correlation length of this feature. In order to test this hypothesis pair distribution function (PDF) analysis was completed to look at the local structures of the materials. Reverse Monte Carlo (RMC) modeling was done on the PDFs of six samples, some which showed intra-chain cation

ordering and dimerization, and some which did not (Fig 3). The results show broad distributions of B - B intra-chain distances for all samples. The widths of these distributions are greater than would be expected from thermal vibrations alone and there are not significant differences in the widths for the different samples (Fig. 4). This supports the idea that dimerization is occurring in all samples on a local level. The PDF data also show that the Al - X distances are longer than the Si - X distances, as indicated by a high- r shoulder on the first peak in the PDF corresponding to B - X distances. This is expected chemically but not apparent from the average structure due to the disorder on the cation sites. No other major local distortions were observed and in general the distance distributions were fairly narrow, indicating that the samples are highly crystalline and the structure type is rigid.

From these observations it appears that there is a weak tendency for Si - Al - Si - Al cation ordering within the edge sharing chains. It is worth noting that while there is variation of the $B9$ and $B10$ occupancies among the eighteen samples studied, the total concentration of Al within the chains is always close to 50%. What varies more is how much is distributed on which site. This can be interpreted as there always being this type of ordering present, along with dimerization, in all samples, but that the correlation length varies between samples. It appears that there are often mistakes or faults in this ordering, preventing the long range translational periodicity that would result in unique crystallographic sites for the two ions, and that the amount of mistakes depends on the exact synthesis conditions or compositions of the sample.

The electronic structure calculations show that having alternating Si - Al - Si - Al chains lowers the total energy of the system relative to having the chains fully occupied by Al or Si . However, an Al - Si - Al - Si ordering is also possible to realize with ~ 1.5 eV/cell higher than the lowest energy structure, and thus the average occupancy of $B9$ and $B10$ does not definitely show the alternating occupancy of Al and Si . We stress that the interatomic correlation between Si and Al , rather than their site occupancy, is essential to find the Si - Al ordering in this system. Quantitatively, the dimerization characterized by the difference between Al - Si bond length and Si - Al bond length in an alternative chain is 0.12 Å. On the other hand, when Al - Al or Si - Si ordering is present within a chain, the difference of the length of neighboring bonds is 0.02 Å. The RMC simulations give values around 0.15 Å, which supports the above interpretation.

3.4. N^{3-}/O^{2-} Ordering. Since it is extremely difficult to prevent the incorporation of some oxygen in the samples, it is important to understand where this oxygen is located in the structure. There are 14 different anion sites in this structure. Twelve of these anions are bonded to three B -cations, while the other two sites are coordinated to only two B -cations. Rietveld refinements were done on the three samples with the highest oxygen contents and all gave similar results. They show that the oxygen is partially ordered onto the two sites which are coordinated to only two B -cations, while the rest is distributed among the other sites.

It was found that about 37% of all the oxygen is located at sites $X9$ and $X14$, which are bonded to only two B -cations. The $X9$ site had an average occupancy of 0.18 and the $X14$ site

had an average occupancy of 0.25. This gives the $X9$ and $X14$ sites 2.5 and 3.5 times more oxygen than would be expected from a random distribution, respectively. This makes sense from a molecular perspective since oxygen generally prefers to make only 2 bonds, while nitrogen generally makes 3. However, the driving force for this ordering is not great enough to lead to complete site ordering as over half the oxygen is still distributed over the other sites. Smaller amounts of oxygen were found to be present on sites $X1$, $X2$, $X3$, $X4$, $X8$, and $X11$. Sites $X5$, $X6$, $X7$, $X10$, $X12$, and $X13$ were found to have very little or no oxygen. Sites $X1$ - $X4$ are the anion sites that make up the edge sharing chains. One reason why these sites might have a preference over the other 3-coordinate X -sites is that the X - X distances within the edge sharing chains are slightly shorter (~ 2.5 Å) than those which are not part of these chains (~ 2.7 - 2.9 Å). The lower charged and smaller O^{2-} would be preferred on these sites compared to N^{3-} . The reasons for a slight preference of sites $X8$ and $X11$ are not clear. The ESDs for the N/O site occupancies were generally 0.01 or 0.02.

Electronic structure calculations were done with the O occupying various sites. Although both $X9$ and $X14$ are doubly coordinated to adjacent B -sites, the calculations show that $X14$ is a more favorable location for oxygen. This is consistent with Rietveld results which show the $X14$ site to be slightly more occupied.

3.5 DFT Results and the Link between Cation and Anion Ordering. The electronic structure calculations were done using various combinations of Si/Al and N/O ordering. Figure 5 shows the calculated total energy of $Sr_2Si_7Al_3ON_{13}$ obtained by varying the atomic configurations with Al occupying three of $B1$, $B7$, $B9$, $B10$, and O occupying either $X9$ or $X14$. The horizontal lines in the figure shows the relative total energy of each configuration and the occupancy of $B9$ and $B10$ are labeled for some low-lying states. The energy difference between the lowest two states is only 1.3 eV/cell, which shows that disorder of the cations and anions can occur easily. Although the origin of the disorder of Si/Al and N/O is not a single factor, this energy level structure is likely relevant to it and can explain why only partial order is observed. As for the electronic state of each configuration, we note that this compound is always insulating, i.e., none of the calculated configurations gives dangling bonds and/or mid-gap states. Figure 6 shows the total density of states for the lowest energy configuration in which we clearly find that a well-defined energy band gap is present. We also note that the band gap energy is about 3.5 eV irrespective of type of cation/anion ordering. Thus, although some mixture of different configurations exists in a sample, it is sufficient to contain the 4f and 5d states of Ce inside the energy band gap, meaning this material is suitable for phosphors for white LEDs.

The cation and anion order do not seem to be completely independent. The preference of oxygen for the $X14$ site over the $X9$ site can be linked to the favorable energy of Al–O bonds over Al–N bonds. The $X9$ anion is bonded to the $B3$ and $B8$ cations. The NPD results show that both these sites are occupied exclusively by Si. On the other hand, the $X14$ anion is bonded to the $B5$ and $B7$ cations and the $B7$ site is found by NPD to be sustainably occupied by Al, leading to an Al–O bond. We mention that the typical values of the bond energies of Al–O, Si–N, Si–O,

Al–N bonds are 5.0 eV, 4.6 eV, 4.6 eV, and 3.1 eV, respectively, which shows that Al–N bond is, in particular, energetically unfavorable amongst the four types of the bonds. Hence, the number of Al–N bonds is minimized in the lowest energy structure. Although this interpretation is rather qualitative, we consider that the *X14* is preferable to *X9* for O when *B7* is occupied by Al.

4. Conclusions

Neutron powder diffraction data and density functional theory calculations on a series of compounds with compositions near $\text{Sr}_2\text{Si}_7\text{Al}_3\text{ON}_{13}$ have shown that the cation and anion ordering in this structure type is more complex than was supposed. The combined NPD and DFT approaches were highly complementary in establishing cation and anion ordering in the $\text{Sr}_2\text{Si}_7\text{Al}_3\text{ON}_{13}$ system. The NPD results guided the choice of possible configurations for the theoretical studies, while the DFT studies confirmed a number of experimental observations. In contrast to what was previously assumed, the chains of edge sharing tetrahedra are not fully occupied by Al, but are about half occupied by Al and half occupied by Si. There is also evidence to suggest that there is a weak tendency for Si–Al ordering within these chains and that there may also be a dimerization occurring to form Si–Al pairs. Two other sites (*B1* and *B7*) are also unexpectedly found to contain significant quantities of Al. The location of oxygen atoms within this structure type has also been addressed for the first time. It is found that the O preferentially occupies the two 2-coordinate anion sites in the structure, but that there is some oxygen distributed on several other sites as well. These results are supported by electronic structure calculations in which the lowest energy state is realized when the Al occupy *B1*, *B7*, and *B10*, while O occupies *X14*. Dimerization into Si–Al pairs in this configuration is also confirmed by the calculations.

Acknowledgements:

This work benefited from the use of the HIPD and NPDF instruments at the Lujan Neutron Scattering Center at Los Alamos Neutron Science Center. Los Alamos National Laboratory is operated by Los Alamos National Security, LLC under DOE Contract No. DE-AC52 06NA25396. Funding for this project was provided by Toshiba Corporation. The authors are also grateful to M. Tohyama and M. Ezaki for valuable discussions.

Site	<i>x</i>	<i>y</i>	<i>z</i>	$U_{\text{iso}} (\text{\AA}^2)$
A(1)	0.2799(3)	0.4924(2)	0.311(1)	0.0350(5)
A(2)	0.3544(3)	0.6954(2)	0.809(1)	0.0350(5)
B(1)	0.3637(5)	0.2788(3)	0.798(2)	0.0130(2)
B(2)	0.0789(4)	0.6995(3)	0.798(2)	0.0130(2)
B(3)	0.1914(5)	0.6369(2)	0.312(2)	0.0130(2)
B(4)	0.0037(5)	0.5423(2)	0.302(1)	0.0130(2)
B(5)	0.5538(5)	0.4697(2)	0.312(1)	0.0130(2)
B(6)	0.3951(5)	0.3459(3)	0.308(2)	0.0130(2)
B(7)	0.1636(5)	0.5656(3)	0.809(2)	0.0130(2)
B(8)	0.4746(4)	0.6080(2)	0.306(2)	0.0130(2)
B(9)	0.1600(6)	0.3496(3)	0.528(1)	0.0130(2)
B(10)	0.1501(6)	0.3510(4)	0.024(1)	0.0130(2)
X(1)	0.0658(2)	0.3169(1)	0.272(1)	0.0150(1)
X(2)	0.2515(2)	0.3740(1)	0.2901(9)	0.0150(1)
X(3)	0.2104(2)	0.2981(1)	0.777(1)	0.0150(1)
X(4)	0.0989(2)	0.3992(1)	0.7694(9)	0.0150(1)
X(5)	0.4057(2)	0.2716(1)	0.4597(9)	0.0150(1)
X(6)	0.3631(2)	0.2075(1)	0.9640(9)	0.0150(1)
X(7)	0.4921(2)	0.3989(1)	0.4579(8)	0.0150(1)
X(8)	0.4391(2)	0.3349(1)	0.9614(9)	0.0150(1)
X(9)	0.3358(2)	0.6333(1)	0.3418(9)	0.0150(1)
X(10)	0.0556(2)	0.5189(1)	0.9818(9)	0.0150(1)
X(11)	0.1597(2)	0.6405(1)	0.9644(8)	0.0150(1)
X(12)	0.1241(2)	0.5746(1)	0.4709(8)	0.0150(1)
X(13)	0.4895(2)	0.5337(1)	0.4674(9)	0.0150(1)
X(14)	0.7038(2)	0.4693(1)	0.346(1)	0.0150(1)

Table 1. The fractional coordinates and ADPs of one for the samples studied. Other structural parameters are $a = 11.7098(2) \text{ \AA}$, $b = 21.4002(3) \text{ \AA}$, $c = 4.9648(1) \text{ \AA}$, $V = 1244.13(2) \text{ \AA}^3$, space group $Pna2_1$, $Z = 4$.

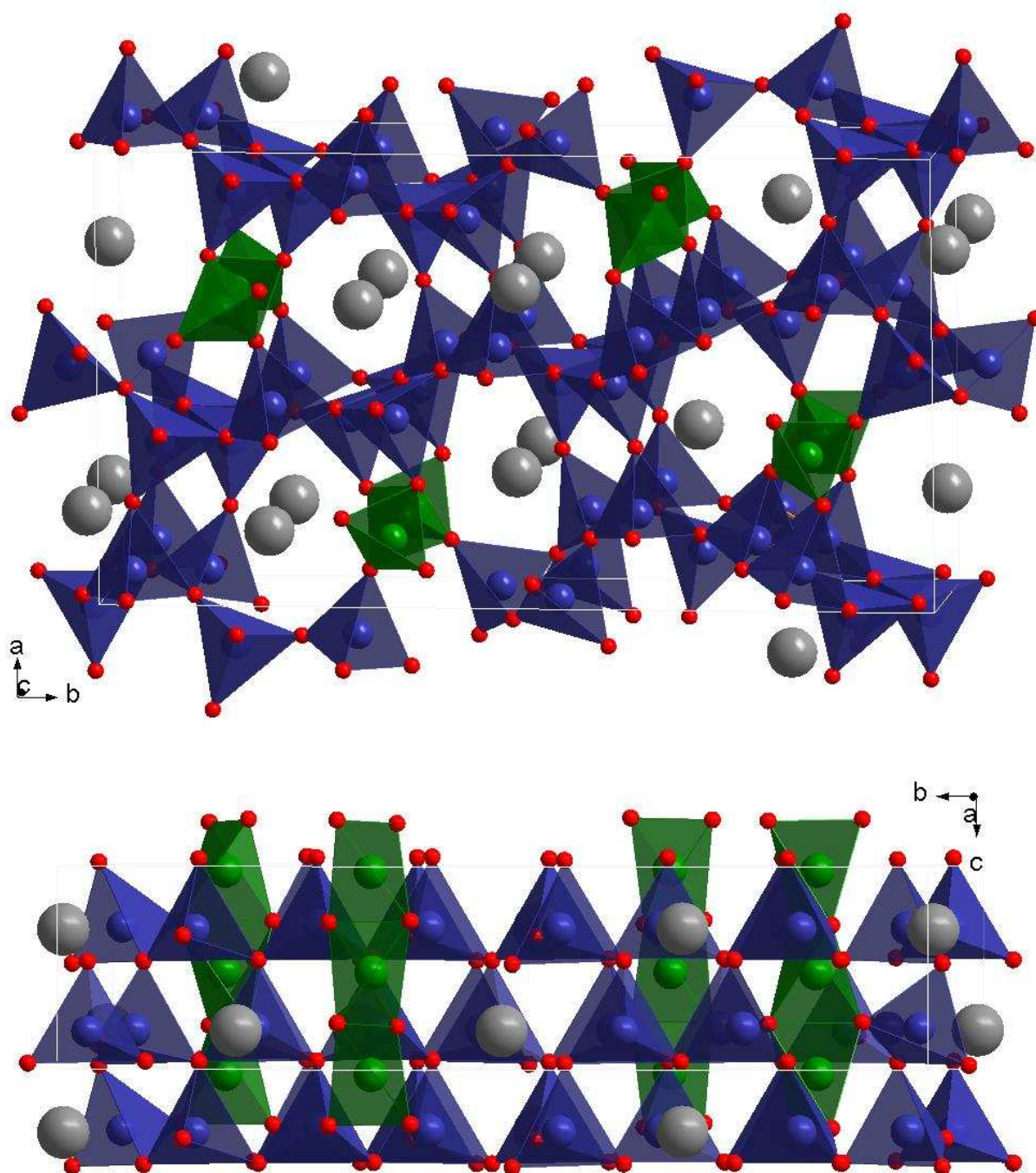


Figure 1. Two views of the $A_2B_{10}X_{14}$ structure type. The A -sites are gray, the B -sites are blue and green, and the X -sites are red. The blue tetrahedra are corner sharing only while the green tetrahedra share edges and corners.

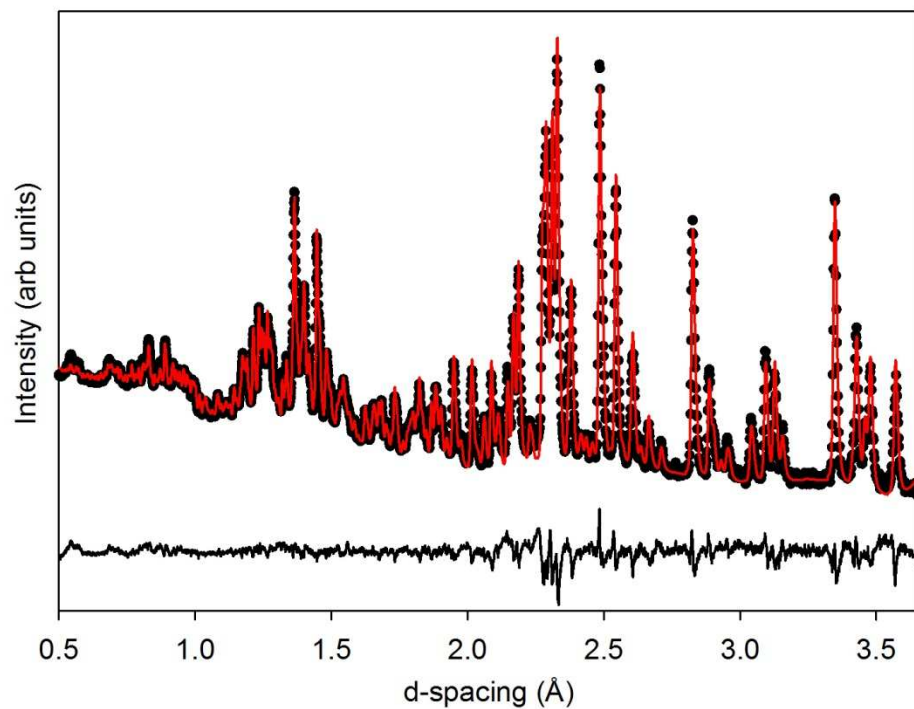


Figure 2. Rietveld refinement of one of the $\text{Sr}_2\text{Si}_7\text{Al}_3\text{ON}_{13}$ samples. The data shown are from bank 1 (153°) of the HIPD instrument. The refinements also used the data from the -153° bank as well as the $\pm 90^\circ$ and $\pm 40^\circ$ banks which cover higher d -spacing. The black dots are the data points, the red line is the fit, and the difference is shown beneath.

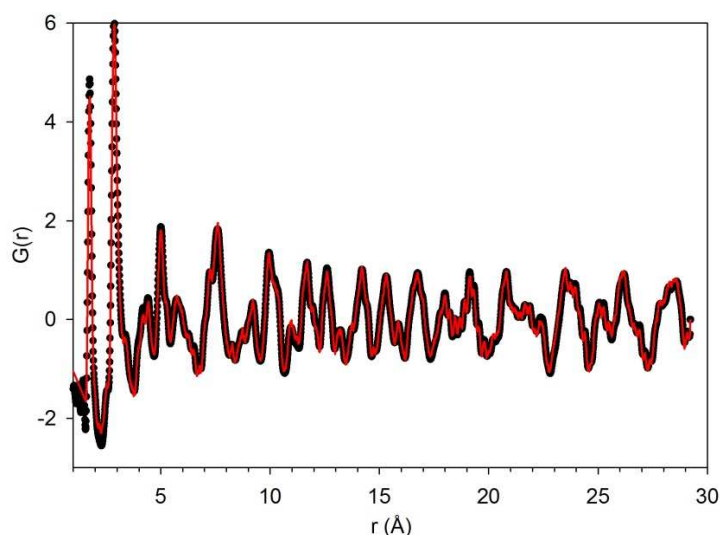


Figure 3. The experimental pair distribution function (black dots) and the fit using an RMC supercell (red) of a $\text{Sr}_2\text{Si}_7\text{Al}_3\text{ON}_{13}$ sample.

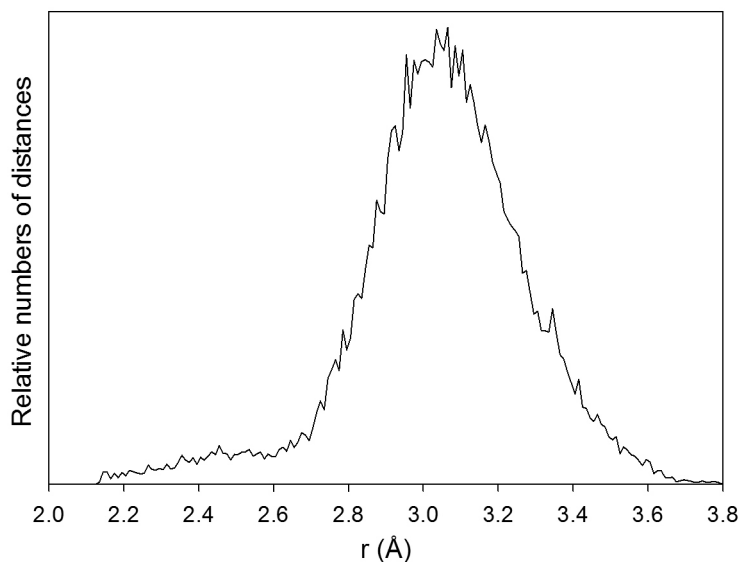


Figure 4. An example of the B - B nearest neighbor distance distribution from RMC modeling of PDF data. The main high- r peak centered at ~ 3.0 Å is from all of the B - B distances involving corner sharing tetrahedra. The low- r feature, between 2.2 Å and 2.7 Å, is from $B9$ - $B10$ distances in the edge sharing chain. Notice how the $B9$ - $B10$ distance distribution is not a sharp peak but rather a broad distribution, supporting the idea of Si-Al dimerization. Similar results were obtained for all 6 samples studied by PDF analysis regardless of whether dimerization was observed in the average crystal structure.

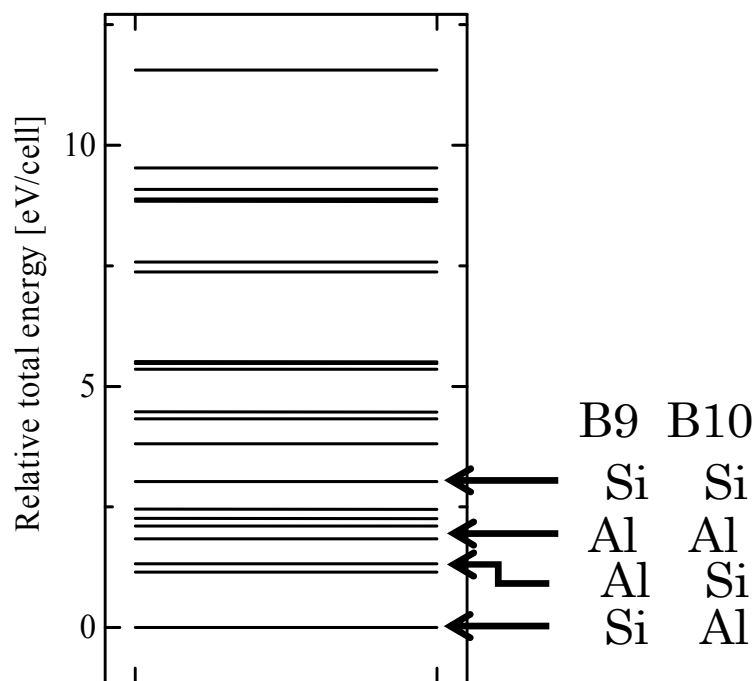


Figure 5. Calculated relative total energies for 24 different configurations of $\text{Sr}_2\text{Si}_7\text{Al}_3\text{ON}_{13}$. $B1$, $B7$, $B10$ are occupied by Al, and $X14$ is occupied by O in the lowest energy state.

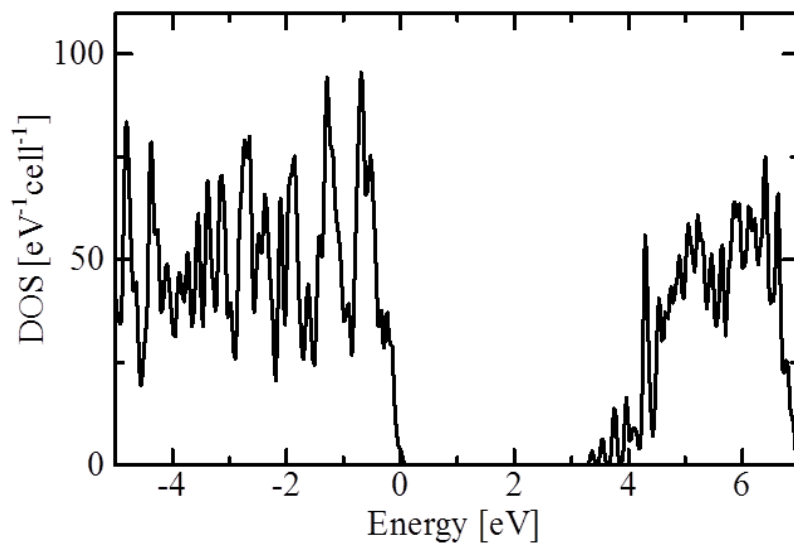
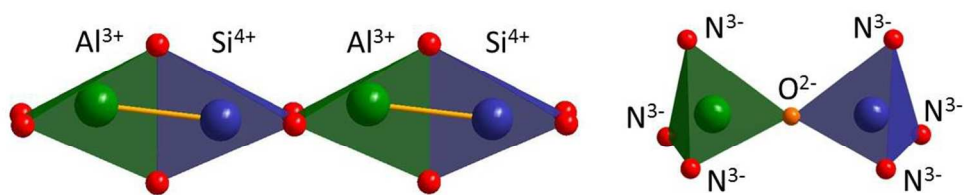


Figure 6. The density of states for the lowest energy configuration of $\text{Sr}_2\text{Si}_7\text{Al}_3\text{ON}_{13}$, showing the material to be an insulator with an energy band gap of approximately 3.5 eV.

References:

1. L. Liu, R.-J. Xie, N. Hirosaki, T. Takeda, C.-n. Zhang, J. Li, and X. Sun, *Sci. Technol. Adv. Mater.*, 2011, **12**, 034404.
2. N. Hirosaki, R.-J. Xie, K. Kimoto, T. Sekiguchi, Y. Yamamoto, T. Suehiro, M. Mitomo, *Appl. Phys. Lett.*, 2005, **86**, 211905.
3. R.-J. Xie, N. Hirosaki, K. Sakuma, Y. Yamamoto, M. Mitomo, *Appl. Phys. Lett.*, 2004, **84**, 5404.
4. Y. Q. Li, N. Hirosaki, R.-J. Xie, T. Takeda, M. Mitomo, *Chem. Mater.*, 2008, **20**, 6704-6714.
5. Y.Q. Li, J. E. J. van Steen, J. W. H. van Krevel, G. Botton, A. C. A. Delsing, F. J. DiSalvo, G. de With, H. T. Hintzen, *J. Alloy Compd*, 2006, **417**, 273-279.
6. W. Li, R.-J. Xie, T. Zhou, L. Liu, Y. Zhu, *Dalton Trans.*, 2014, **43**, 6132.
7. Y. Fukuda, K. Ishida, I. Mitsuishi, S. Nunoue, *Appl. Phys. Express*, 2009, **2**, 012401.
8. C. Hecht, F. Stadler, P. J. Schmidt, J. Schmedt auf der Gunne, V. Baumann, W. Schnick, *Chem. Mater.*, 2009, **21**, 1595-1601.
9. J. Ruan, R.-J. Xie, N. Hirosaki, T. Takeda, *J. Am. Ceram. Soc.*, 2011, **94**, 536-542.
10. J. Ruan, R.-J. Xie, S. Funahashi, Y. Tanaka, T. Takeda, T. Suehiro, N. Hirosaki, Y.-Q. Li, *J. Solid State Chem.*, 2013, **208**, 50-57.
11. Z. Zhnag, O. M. ten Kate, A. C. A. Delsing, Z. Man, R.-J. Xie, Y. Shen, M. J. H. Stevens, P. H. L. Notten, P. Dorenbos, J. Zhao, H. T. Hintzen, *J. Mater. Chem. C*, 2013, **1**, 7856-7865.
12. L. Zhang, J. Zhang, X. Zhang, Z. Hao, H. Zhao, Y. Luo, *ACS Appl. Mater. Interfaces*, 2014, **5**, 12839-12846.
13. Y. Fukuda, A. Okada, A. K. Albessard, *Appl. Phys. Express*, 2012, **5**, 062102.
14. A. C. Larson and R. B. Von Dreele, Los Alamos National Laboratory Report No. LAUR 86-748, 2004.
15. B. H. Toby, *J. Appl. Crystallogr.*, 2001, **34**, 210.
16. P. F. Peterson, M. Gutmann, Th. Proffen and S.J.L. Billinge, *J. Appl. Crystallogr.*, 2000, **33**, 1192.
17. M. G. Tucker, D. A. Keen, M. T. Dove, A. L. Goodwin, Q. Hui, *J. Phys.: Condens. Matter*, 2007, **19**, 335218.

18. P. Hohenberg and W. Kohn, *Phys. Rev.*, 1964, **136**, B864.
19. J. P. Perdew and Y. Wang, *Phys. Rev.*, 1965, **140**, A1133.
20. D. Vanderbilt, *Phys. Rev. B*, 1990, **41**, 7892.



194x43mm (150 x 150 DPI)